

Nanoscale phase separation in $\text{La}_{0.7}\text{Ca}_{0.3}\text{MnO}_3$ films: evidence for texture-driven optical anisotropy

This article has been downloaded from IOPscience. Please scroll down to see the full text article.

2003 J. Phys.: Condens. Matter 15 2635

(<http://iopscience.iop.org/0953-8984/15/17/317>)

View [the table of contents for this issue](#), or go to the [journal homepage](#) for more

Download details:

IP Address: 171.66.16.119

The article was downloaded on 19/05/2010 at 08:51

Please note that [terms and conditions apply](#).

Nanoscale phase separation in $\text{La}_{0.7}\text{Ca}_{0.3}\text{MnO}_3$ films: evidence for texture-driven optical anisotropy

A S Moskvin¹, E V Zenkov¹, Yu P Sukhorukov², E V Mostovshchikova²,
N N Loshkareva², A R Kaul³ and O Yu Gorbenko³

¹ Ural State University, 620083 Ekaterinburg, Russia

² Institute of Metal Physics, Ural Division of the Russian Academy of Sciences,
620219 Ekaterinburg, Russia

³ Moscow State University, 119899 Moscow, Russia

E-mail: eugene.zenkov@usu.ru

Received 27 January 2003

Published 22 April 2003

Online at stacks.iop.org/JPhysCM/15/2635

Abstract

The infrared optical absorption ($0.1 \text{ eV} < \hbar\omega < 1.5 \text{ eV}$) in $\text{La}_{0.7}\text{Ca}_{0.3}\text{MnO}_3$ films on LaAlO_3 substrates exhibits a drastic temperature evolution of the spectral weight, evidencing an insulator-to-metal transition. Single-crystal films were found to reveal strong linear dichroism with anomalous spectral oscillations and fairly weak temperature dependence. Starting from the concept of phase separation, we develop an effective medium model to account for these effects. The optical anisotropy of the films is attributed to the texturization of the ellipsoidal inclusions of the quasimetal phase caused by a mismatch of the film and substrate and the twin texture of the latter.

1. Introduction

The investigation of doped rare-earth manganites has a long history, starting in the 1950s. The intensive research of the last decade, stimulated by the discovery of colossal magnetoresistance, has significantly enriched our understanding of these systems. However, recent studies argue its internal nature to be far more complex than what is predicted by the conventional phase diagrams [1, 2]. In particular, there is growing experimental evidence [3–5] of a generic nanoscale inhomogeneity of manganites as well as many other strongly correlated transition metal oxides [6, 7].

Infrared (IR) optical studies [8] of $\text{La}_{1-x}\text{Ca}_x\text{MnO}_3$ ($0.1 < x < 0.8$) were among the first investigations to reveal phase separation in manganites. The analysis of diffuse neutron scattering studies of spin correlations in $\text{La}_{1-x}\text{Ca}_x\text{MnO}_3$ ($x < 0.2$) single crystal [9] confirms the existence of ferromagnetic (FM) inhomogeneities below T_C in the form of platelets with a mean diameter of about 16 \AA .

In the films, unlike in the bulk samples, the phase-separated state can persist at still higher doping, probably due to the specific properties of the film–substrate interface stabilizing the novel phase. Indeed, atomic force microscopy of $\text{La}_{0.67}\text{Ca}_{0.33}\text{MnO}_3$ films deposited on LaAlO_3 substrates [5] yields a direct visualization of coexisting FM metallic and charge-ordered insulating phases. The authors of [5] suggest that the key factor governing the occurrence of this phase separation is the mismatch of the film and substrate, resulting in nonuniform compressive strains of the lattice and concomitant inhomogeneities in the exchange and hopping parameters. The low-strain well-conducting islands with mean size as large as 500 Å, separated by high-strain insulating interfaces, are clearly discernible in the micrographs of the film.

In this paper we present the results of optical studies of strained $\text{La}_{0.7}\text{Ca}_{0.3}\text{MnO}_3$ films, that can be considered as another possible manifestation of intrinsic phase inhomogeneity of these systems. Surprisingly, the IR absorption spectra display significant optical anisotropy and unusual oscillating frequency dependence of the dichroism, that cannot be associated with certain electronic transitions. Our model calculations, based on the concept of strain-induced ordering of prolate quasimetal droplets in the parent insulator, agree quantitatively with experiment.

2. Experimental details

Two $\text{La}_{0.7}\text{Ca}_{0.3}\text{MnO}_3$ (LCMO) manganite films, 60 and 300 nm in thickness, were grown on single-crystalline (001)-oriented LaAlO_3 (LAO) substrates. The details of the film growth and sample characterization are given elsewhere [10, 11]. The x-ray diffraction patterns and high-resolution transmission electron microscopy confirm the epitaxial character of the films. Rocking curve methods yield $\text{FWHM} = 0.16^\circ$, which implies a small mosaicity and high-quality orthorhombic $Pnma$ structure of the films. The out-of-plane lattice constants c (3.870 Å (60 nm) and 3.872 Å (300 nm)) are close to the in-plane ones (3.863 Å (60 nm) and 3.862 Å (300 nm)) for both films, so the structural anisotropy is small. We note a small amount of Mn_3O_4 impurity in the thick (300 nm) film, that does not alter the perovskite structure of the sample and is observed in the form of nanoscale embeddings in the epitaxial matrix.

The optical experiments were performed over the ranges of $0.1 < \hbar\omega < 1.5$ eV, $80 < T < 295$ K, using an automatic prismatic spectrometer. The absorption coefficient (K) was derived from the measured ratio of transmitted to incident beam intensities as $K = (1/d) \ln((1-R)^2 I_0/I)$, d and R being the film thickness and the reflectance, respectively. A grating polarizer was employed in the IR region. The spectra were taken with the light wave \mathbf{E} -vector adjusted along and normally to the direction of maximal absorption (c -axis), achieved by the rotation of the polarizer. As usual, the linear dichroism is defined as

$$\Delta = \frac{K(\mathbf{E} \parallel c) - K(\mathbf{E} \perp c)}{K(\mathbf{E} \parallel c) + K(\mathbf{E} \perp c)}, \quad (1)$$

where the K s are the absorption coefficients for appropriate polarizations.

3. Results and discussion

3.1. Optical spectra

The IR optical responses of doped manganites such as $\text{La}_{1-x}(\text{Sr}, \text{Ca})_x\text{MnO}_3$ differ strongly from those of the pure LaMnO_3 system. A self-consistent description of the charge-transfer (CT) bands in LaMnO_3 [12] shows a multi-band structure of the CT optical response with the weak low-energy edge at 1.7 eV, associated with a forbidden $t_{1g}(\pi)$ – e_g transition.

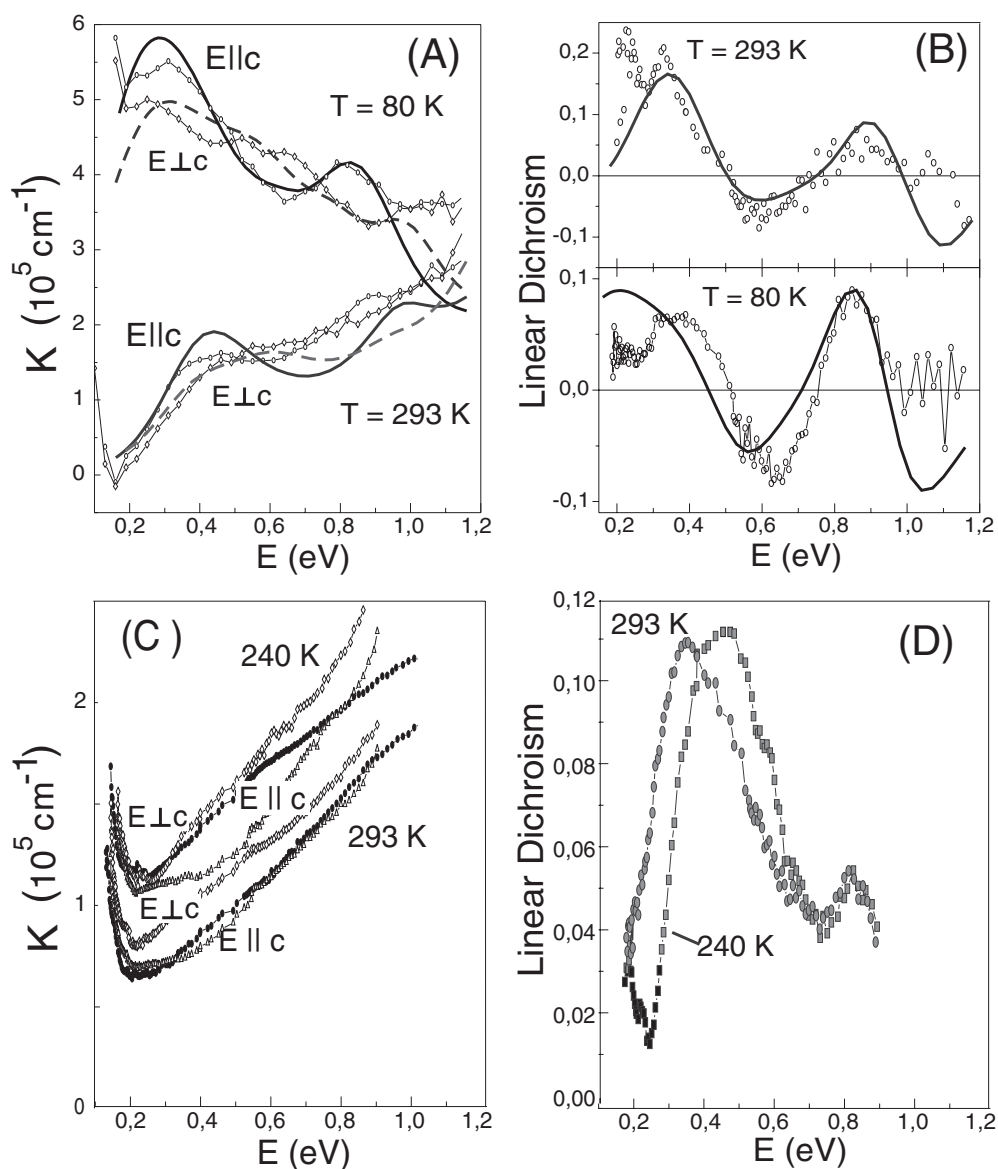


Figure 1. Top panel: spectroscopic data for thin (60 nm) $\text{La}_{0.7}\text{Ca}_{0.3}\text{MnO}_3$ film at $T = 80$ and 293 K. (A) Absorption spectra for two polarizations: experimental data are shown by dots; curves are the result of fittings in the framework of EMT (the unpolarized light spectra are not shown). (B) Linear dichroism spectra: experiment (dots) and EMT (curves). Bottom panel: spectroscopic data for thick (300 nm) $\text{La}_{0.7}\text{Ca}_{0.3}\text{MnO}_3$ film at $T = 240$ and 293 K. (C) Absorption spectra: unpolarized light (circles), $E \parallel c$ polarization (triangles), $E \perp c$ polarization (diamonds). (D) Linear dichroism spectra.

These predictions are in good agreement with experimental spectra. A common feature of doped manganites and related systems is revealed in an unconventional enhancement of the IR spectral weight, evidencing the appearance of a free charge-carrier contribution.

The absorption spectra of a thin (60 nm) film are shown in figure 1(A). At $T = 295$ K the unpolarized light IR spectrum displays an insulating gap-like behaviour. However, this

behaviour is unusual, since the absorption, without being metallic, remains rather large over the entire spectral range. The increase of the absorption coefficient below a dip near 0.2 eV is related to phonon bands, starting at ~ 0.09 eV,

The lowering of the temperature to 80 K, well below the Curie temperature $T_C \approx 268$ K, entails a drastic enhancement of the IR spectral weight, straightforwardly evidencing the appearance of a free charge-carrier contribution. The very large free carrier absorption of thick (300 nm) film at $T = 80$ K makes transmission experiments difficult, so in the FM region the measurements were performed only around T_C (figure 1(C)). We observed quite similar behaviour also for self-doped $\text{La}_{0.83}\text{MnO}_3$ [13] and $\text{La}_{0.7}\text{Sr}_{0.3}\text{MnO}_3$ films [14]. Comparative analysis of these spectra and those of other doped manganites ($\text{La}_{1-x}(\text{Sr}, \text{Ca})_x\text{MnO}_3$ [15, 16], $\text{Nd}_{1-x}\text{Sr}_x\text{MnO}_3$ [17], etc) allows us to conclude that here we are dealing with seemingly universal physical behaviour, common to a wide family of doped manganites. Earlier, we assigned [13, 18, 19] this unconventional optical response to the nanoscopically inhomogeneous texture of manganites, which looks like a system of metallic droplets in an insulating matrix. The spectral features are believed to be governed mainly by the temperature-dependent metallic volume fraction and geometrical resonances in a nanoscopically inhomogeneous system. From the theoretical standpoint, the possibility of phase separation in manganites was examined in pioneering work by Nagaev [20], and subsequently developed further [21]. It was shown that the competition of hopping energy and double exchange render the charge-carrier segregation in nanoscopic FM conducting droplets (ferrons) energetically favourable as compared to the uniform spin-canted state. Such a segregation is accompanied with a gradual shift of the spectral weight from the absorption bands of the parent AF matrix to lower-energy excitations in the droplets of a novel phase.

The experiments in polarized light revealed interesting features, observed in IR absorption spectra of thin film both in FM and paramagnetic (PM) states, namely oscillations about the unpolarized light spectrum (figure 1(A)). The spectra of thick films look different (figure 1(C)). Above T_C , the absorption coefficient in $\mathbf{E} \perp c$ polarization exceeds in magnitude that for unpolarized light, while in $\mathbf{E} \parallel c$ polarization these spectra nearly coincide over the range 0.2–0.9 eV. In the FM state (240 K), the $\mathbf{E} \perp c$ and unpolarized spectra are indistinguishable in the 0.2–0.5 eV range, but above 0.5 eV the absorption coefficient in the $\mathbf{E} \perp c$ polarization shows a more rapid increase. The $\mathbf{E} \parallel c$ spectrum approaches the unpolarized one from below and intersects with it at 0.8 eV.

The above peculiarities of polarized light absorption manifest themselves in the spectral oscillations of the linear dichroism of thin films with an amplitude of the order of 0.3 about zero (figure 1(B)). The dichroism in thick films is positive throughout the spectral range 0.2–0.9 eV with two peaks, at 0.4 and 0.8 eV, whose positions are close to those observed in the dichroism spectrum for thin films (figure 1(D)). It should be noted that upon cooling from $T = 293$ to 240 K, the low-energy peak blue-shifts from 0.35 to 0.45 eV.

3.2. Discussion

Nontrivial questions arise about the origin of the observed peculiarities of the optical response, since no allowed electric dipole transitions are known to fall in the spectral range under consideration. As a result of the twinning, the LAO substrate reveals itself to have optical anisotropy. However, the magnitude of its dichroism is quite small as compared with that observed for LCMO/LAO films (figure 2).

While the magnitude of the absorption coefficient for the films varies by hundreds of per cent upon cooling from $T \sim 293$ K to $T = 80$ K, the behaviour of the dichroism remains practically unchanged both in PM and FM states, and its amplitude does not change significantly

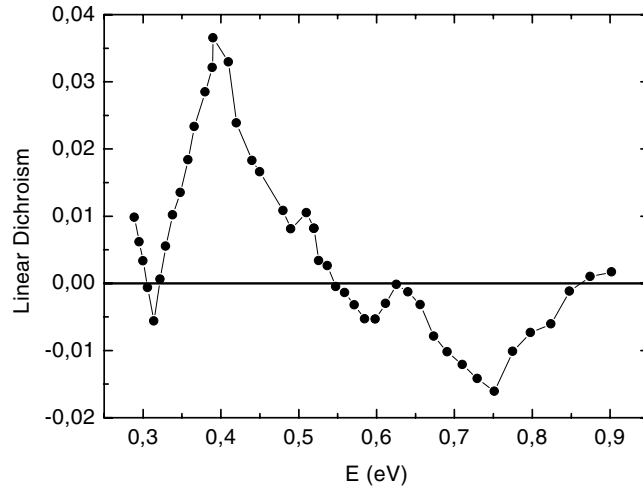


Figure 2. The linear dichroism of the LAO substrate.

when changing from a thin film to a thick one. Note that the dichroism is observed in both films and thus is not related to Mn_3O_4 impurity effects. However, if we restrict consideration to conventional explanations, we may overlook other possibilities, stemming from the intrinsic nanoscale phase inhomogeneity of doped manganites. In particular, we assume that, under the mismatch-induced nonuniform stresses, the droplets of the quasimetallic phase may align to form a structure somewhat like a nematic liquid crystal. Such a texture, reflecting the twin pattern of the substrate, results in a significant enhancement of the observed dichroism of the LCMO/LAO films. We show that this model, which is an extension of our general approach to manganites considered as nanoscopically inhomogeneous systems [13, 18, 19], can provide a good quantitative agreement with all the experimental findings presented in the previous section.

First, we would like to briefly overview effective medium theory (EMT) [22], which appears to be a powerful tool for quantitative description of the optical response of inhomogeneous systems. In its simplest form, the EMT equation for the effective dielectric function ε_{eff} of the two-component inhomogeneous system reads as follows [22]:

$$\int_V dV p(\varepsilon) \sum_{i=1}^3 \frac{\varepsilon - \varepsilon_{eff}}{\varepsilon_{eff} + L_i(\varepsilon - \varepsilon_{eff})} = 0, \quad (2)$$

where the integration runs over the volume of the sample, $p(\varepsilon) = p_1\delta(\varepsilon(r) - \varepsilon_1) + p_2\delta(\varepsilon(r) - \varepsilon_2)$. We consider the two components of the binary composite on an equal footing, with $p_{1,2}$ being the volume fractions, and $\varepsilon_{1,2}$ and L_i the dielectric functions and the depolarization factors of the grains of its constituents, respectively.

It is worth emphasizing that in the effective medium approximation the volume of the droplet does not enter the calculations, but is accounted for implicitly in the validity range of the theory, restricting the mean size of the droplet to being smaller than the wavelength. Hence, within the EMT, the volume fractions $p_{1,2}$ can only change through change of the number of droplets rather than due to the variation of their sizes. In general, $p_{1,2}$ are determined by thermodynamical conditions and depend on temperature, pressure, and other external factors. The approach [23] that we employed here to lend more plausibility to this physically transparent EMT scheme is that of taking into account the natural difference between the core and the

surface properties of the inclusions using the standard expression for the polarizability of the coated ellipsoid [24].

The spectra of nanoscopically disordered media display some specific features due to geometric resonances [22] that have no counterpart for homogeneous systems. These arise as a result of resonant behaviour of local field corrections to the polarizability of the granular composite and are governed to a considerable extent by the shape of the grains. The frequency of the geometric resonance is then easily obtained as the one at which the polarizability of small particles diverges. For the case of spherical metallic droplets embedded in an insulating matrix with dielectric permittivity ε_d , this leads to the equation

$$\varepsilon(\omega)_{part} + 2\varepsilon_d = 0, \quad (3)$$

whence the resonance frequency is

$$\omega_r = \frac{\omega_p}{\sqrt{1 + 2\varepsilon_d}}, \quad (4)$$

if Drude's expression with the plasma frequency ω_p is assumed for the metallic permittivity and ε_d is constant. In the case of an arbitrary ellipsoid there are three different principal values of the polarizability and the latter formula generalizes to

$$\omega_r^i = \omega_p \sqrt{\frac{L_i}{\varepsilon_d - L_i(\varepsilon_d - 1)}}, \quad i = 1, 2, 3, \quad (5)$$

where L_i are three shape-dependent depolarization factors. For the cubic matrix it is natural to assume these ellipsoidal droplets to be oriented along main symmetry directions such as [111], [100].

Such a simple model of phase separation enables us to understand the nature of the linear dichroism observed in LCMO/LAO films both above and below T_C even without making any assumptions concerning the intrinsic electronic anisotropy of the constituents. Indeed, for a bulk manganite crystal with cubic symmetry, all orientations of ellipsoidal droplets such as [111] are energetically equivalent and equally distributed, which restores the high degree of symmetry of the system as a whole and results in the optical isotropy of the nanoscopically phase-separated sample. However, any anisotropic noncubic perturbation such as strain lifts the orientational degeneracy of ellipsoidal droplets and gives rise to a certain texture. When this texture is irradiated by a plane wave, the geometric resonances (equation (5)) will be excited selectively depending on the polarization. Thus, the phase-separated sample as a whole can exhibit sizable optical anisotropy in the spectral range of the geometric resonances. Such a situation is likely to occur in our samples due to the unavoidable mismatch of the film and the substrate that generally results in nonuniform strains, which can favour some ordering of the droplets to form a texture. Since the film and the substrate have the same lattice structure, their mismatch would in principle result in bulk contraction, changing the volume of the unit cell. The manganite films grown on LAO substrates are known [25] to be under compressive stress, their lattice being contracted in the plane and expanded in the normal direction. The high energy cost of this deformation makes more feasible the relaxation channel that implies a nonuniform distribution of the metal volume fraction with the density enhanced near the LCMO/LAO interface. Indeed, the smaller volume of the unit cell for the metallic phase as compared with the insulating LCMO matrix provides optimal relaxation of the mismatch. However, the large density of metallic ellipsoidal droplets implies ordering or packing along one of four equivalent directions in the plane of the film. In our case this direction is likely to be determined by the twin texture observed for LAO substrates. In this way, we come to the nucleation of the three-dimensional texture of metallic ellipsoidal droplets resulting in the optical anisotropy of the film. Our preliminary experimental examinations of the optical

anisotropy of the twinned single-crystalline $\text{La}_{0.93}\text{Ce}_{0.07}\text{MnO}_3$ sample also argue in favour of this picture. Note that in all cases the resulting deformation of the lattice may be too small to be detected by conventional x-ray methods.

To check the validity of the hypothesis of the texture-driven dichroism in LCMO/LAO films we simply assumed the nanoparticles to be identically aligned along the optical axis in the plane of the film, so that the amplitude of the dichroism would be governed only by their shape anisotropy. To this end, leaving only one of the terms in the sum (equation (2)), we are in a position to calculate the eigenvalues of the effective dielectric tensor and to simulate the dichroism. To make the model more realistic we assume the metallic-like droplet to take the form of a coated ellipsoid whose dielectric function can be written as follows [24]:

$$\hat{\epsilon}_i = \epsilon_{out} \frac{(\epsilon_{in} - \epsilon_{out})(f L_i^{out} - L_i^{in} - f) - \epsilon_{out}}{(\epsilon_{in} - \epsilon_{out})(f L_i^{out} - L_i^{in}) - \epsilon_{out}}, \quad (6)$$

where the L s are the depolarization factors of inner (*in*) and outer (*out*) confocal shells (core and coating, respectively); f is the core-to-coating volume ratio for this composite inclusion. Leaving aside the question of the microscopic electronic structure of the droplet, we described its core and the coating by the Drude formula:

$$\epsilon = \epsilon_0 - \frac{\omega_p^2}{\omega(\omega + i\gamma)} \quad (7)$$

where ω_p is the plasma frequency, γ is the damping parameter. This approximation is reasonable and is more general than it may seem, since the Drude form can be regarded as a limiting form of the universal expression for dynamical conductivity in terms of the memory function [26] with ω_p and γ as effective parameters. The imaginary part of the dielectric function of LaMnO_3 was fitted to experiment [15] as the sum of three Gaussians over a broad spectral range to ensure the validity of its real part, derived via Kramers–Kronig transformation. Note that the phonon bands have been neglected throughout the calculations. The energies, intensities, and damping constants (ω and γ being in electronvolts) of the Gaussians are $(\omega, I, \Gamma) = ((2.5, 2.6, 0.777), (5.0, 7.8, 0.929), (6.5, 2.866, 0.697))$.

The main results of our calculations are shown in figures 1(A), (B). The room temperature spectra were fitted, given the following parameters: the volume fraction of quasimetal phase $p = 0.1$, $f = 0.4$, $\omega_{p1} = 3.0$ eV, $\omega_{p2} = 1.35$ eV, $\gamma_1 = 0.3$ eV, $\gamma_2 = 0.4$ eV, where the indices 1, 2 stand for the core and the coating of the quasimetal droplet, respectively. The ratio of in-plane semiaxes of quasimetal inclusions is set equal to $\alpha = b/a = 0.5$ and the ratio of out-of-plane to major in-plane semiaxes is set equal to $\beta = c/a = 0.42$. In principle, the quantum size effect in a small nonspherical particle would bring about an anisotropic contribution to the relaxation rate γ . For the sake of simplicity, we neglected this small effect in our model calculations.

As follows from the experiment, the lowering of the temperature shifts the phase equilibrium toward ‘metallization’, drastically expanding the volume fraction of the metallic droplets. However, while the system becomes more metallic, this may not necessarily be the case for an individual droplet because of the noise—the random overlaps with neighbour droplets introduced in its surrounding; so the volume of the core relative to the fluctuating edge region may even get smaller. To simulate the low-temperature spectra, we modified the parameters (α and β kept fixed) as follows: $p = 0.55$, $f = 0.23$, $\omega_{p1} = 2.4$ eV, $\omega_{p2} = 1.12$ eV, $\gamma_1 = 0.3$ eV, $\gamma_2 = 0.3$ eV. Thus, for a fixed doping, the temperature appears to be the main physical parameter, governing the metallic volume fraction and percolation. The intrinsic ‘electronic’ parameters such as ω_p and γ are, roughly speaking, temperature independent with an accuracy of the order of 10–20%. Both results suggest a sound structure

for our simple model. Although it can hardly provide the excellent fit to experiment throughout the entire spectral range, it still captures the essential features of the dichroism spectrum despite a great body of simplifying assumptions. The two-peaked structure of the absorption coefficients, that combine according to equation (1) to provide the oscillations of the dichroism, results from the superposition of geometric (Mie) resonances, governed by a fine tuning of the parameters. It should be noted that the model can yield rather complex behaviour of the spectra with multiple resonances. At the same time, it is worth noting that similar calculations with simple ellipsoidal particles fail to reproduce all the peculiarities of the absorption and dichroism spectra. This means that one should take care with the internal structure of the nanoparticles when employing the EMT in realistic models.

In conclusion, we have reported IR transmission measurements on LCMO films grown on LAO substrates. Upon cooling from room temperature to $T = 80$ K, the absorption coefficient for thin films was found to rise markedly. The main finding of the present studies is the unconventionally large nearly temperature-independent linear dichroism of the films, and its spectral oscillations, unexpected in view of the good structural perfection of the samples. We assert these features to be the manifestation of the inhomogeneous phase-separated state of the films. The optical anisotropy of the film is attributed to the texturization of the ellipsoidal nanoparticles of the quasimetal phase caused by a mismatch of the film and substrate and the twin texture of the latter. The simulation in the framework of an effective medium model provided a good description of experiment. Despite this, at present we cannot exclude other possible scenarios for the linear dichroism in manganite films—in particular, the magnetic one. Indeed, our model implies intrinsic FM ordering of quasimetallic droplets with superparamagnetic behaviour at $T > T_C$ and magnetic percolation below T_C . Such a FM droplet would manifest a magnetic linear dichroism irrespective of its shape. However, for the film to reveal linear dichroism, we need its relevant magnetic texture, or some kind of ordering of the droplets. One should note that, similarly to in our model, a quantitative description of the magnetic mechanism may be given in the framework of the EMT. In fact, the distinction between two mechanisms needs further study.

In any case, we see that the analysis of the optical anisotropy provides an effective tool for examination of the nanoscale texture of the film. More generally, we suggest that the results of the present paper as well as a great body of previous contributions [5, 6, 9, 13] must enrich and extend the conventional understanding of the optical response of manganites, demonstrating the importance of specific effects of its intrinsic nanoscale phase inhomogeneity. In particular, we may state that the specific properties of the dichroism in the spectral range $0.1 \text{ eV} < \hbar\omega < 1.5 \text{ eV}$ support our model [13, 18, 19] in which the appropriate optical response is governed mainly by the geometrical resonances in the nanoscale inhomogeneous system.

Acknowledgments

The work was supported by INTAS 01-0654, Federal programme (contract No 40.012.1.1.1153-14/02), grants RFBR No 01-02-96404, No 02-02-16429, RFMC No E00-3.4-280, E02-3.4-392, CRDF No REC-005 and UR 01.01.042.

References

- [1] Urushibara A *et al* 1995 *Phys. Rev. B* **51** 14103
- [2] Schiffer P, Ramirez A P, Bao W and Cheong S-W 1995 *Phys. Rev. Lett.* **75** 3336
- [3] Nagaev E L 1996 *Usp. Fiz. Nauk* **166** 833 (Engl. transl. 1996 *Phys.-Usp.* **39** 781)

-
- [4] Salamon M B and Jaime M 2001 *Rev. Mod. Phys.* **73** 583
 - [5] Biswas A *et al* 2000 *Phys. Rev. B* **61** 9665
Biswas A *et al* 2001 *Phys. Rev. B* **63** 184421
 - [6] Pan S H *et al* 282 *Nature* **413**
 - [7] Uehara M, Mori S, Chen C H and Cheong S-W 1999 *Nature* **399** 560
 - [8] Loshkareva N N *et al* 1999 *JETP Lett.* **68** 97
 - [9] Biotteau G *et al* 2001 *Phys. Rev. B* **64** 104421-1
 - [10] Gorbenko O Yu, Kaul A R, Babushkina N A and Belova L M 1997 *J. Mater. Chem.* **7** 747
 - [11] Gorbenko O Yu, Graboy I E, Kaul A R and Zandbergen H W 2000 *J. Magn. Magn. Mater.* **211** 97
 - [12] Moskvina A S 2002 *Phys. Rev. B* **65** 205113
 - [13] Sukhorukov Yu P, Loshkareva N N, Mostovshchikova E V, Moskvina A S and Zenkov E V 2003 *JETP* **6** 257
 - [14] Loshkareva N N *et al* 1999 *Phys. Solid State* **41** 426
 - [15] Takenaka K *et al* 1999 *J. Phys. Soc. Japan* **68** 1828
 - [16] Jung J H *et al* 1997 *Phys. Rev. B* **55** 15489
 - [17] Lee H J *et al* 1999 *Phys. Rev. B* **60** 5251
 - [18] Moskvina A S, Zenkov E V and Panov Yu D 2002 *Phys. Solid State* **44** 1519
 - [19] Sukhorukov Yu P *et al* 2001 *JETP* **92** 462
 - [20] Nagaev E L 1972 *Pis. Zh. Eksp. Teor. Fiz.* **16** 558
 - [21] Khomskii D I 2000 *Physica B* **280** 325
Kagan M Yu, Khomskii D I and Mostovo M V 1999 *Eur. J. Phys. B* **12** 217
 - [22] Bergman D J and Stroud D 1992 *Solid State Physics* vol 46, ed H Ehrenreich and D Turnbull (New York: Academic Press) p 148
 - [23] Sheng P 1980 *Phys. Rev. Lett.* **45** 60
 - [24] Bilboul R R 1969 *J. Phys. D: Appl. Phys.* **2** 921
 - [25] Prellier W, Lecœur Ph and Mercey B 2001 *J. Phys.: Condens. Matter* **13** R915
 - [26] Götze W and Wölfle P 1972 *Phys. Rev. B* **6** 1226